Supplement to: Linking stratosphere–troposphere coupling biases to Annular Mode predictability and midlatitude impacts in subseasonal forecast systems

Chaim I. Garfinkel[1], Zachary D. Lawrence[2,3], Amy H. Butler[4], Blanca Ayarzagüena[5,6], Marta Abalos[5], David Barriopedro[6], Natalia Calvo[5,6], Alvaro de la Cámara[5], Andrew Charlton-Perez[7], Judah Cohen[8], Ying Dai[9], Daniela I.V. Domeisen[10], Etienne Dunn-Sigouin[11], Irene Erner[12], Javier García-Serrano[13], Neil P. Hindley[14], Peter Hitchcock[9], Martin Jucker[15], Alexey Yu. Karpechko[12], Hera Kim[16], Gerbrand Koren[17], Simon H. Lee[18], Robert W. Lee[7], Marisol Osman[19,20], Froila M. Palmeiro[13], Jian Rao[21], Chen Schwartz[1,22], Seok-Woo Son[16], Corwin J. Wright[14], and Rachel W.-Y. Wu[23]

[1]Fredy & Nadine Herrmann Institute of Earth Sciences, The Hebrew University of Jerusalem, Israel
[2]Cooperative Institute for Research in Environmental Sciences (CIRES), University of Colorado Boulder, Boulder, CO, USA
[3]NOAA Physical Sciences Laboratory (PSL), Boulder, CO, USA
[4]NOAA Chemical Sciences Laboratory (CSL), Boulder, CO, USA
[5]Department of Earth Physics and Astrophysics, Universidad Complutense de Madrid, Madrid, Spain
[6]Instituto de Geociencias (IGEO), Consejo Superior de Investigaciones Científicas – Universidad Complutense de Madrid (CSIC-UCM), Madrid, Spain.
[7]Department of Meteorology, University of Reading, Reading, UK
[8]Atmospheric and Environmental Research Inc., Lexington, MA, USA.
[9]Dept. Earth and Atmospheric Sciences, Cornell University, Ithaca, NY, USA
[10]University of Lausanne, Lausanne, Switzerland
[11]NORCE Norwegian Research Centre and Bjerknes Centre for Climate Research, Bergen, Norway
[12]Finnish Meteorological Institute, Meteorological Research, Helsinki, Finland
[13]Group of Meteorology, Universitat de Barcelona (UB), Barcelona, Spain
[14]Centre for Climate Adaptation and Environment Research, University of Bath, Bath, UK
[15]Climate Change Research Centre and ARC Centre of Excellence for the Weather of the 21st Century, University of New South Wales, Sydney, Australia
[16]School of Earth and Environmental Sciences, Seoul National University, South Korea
[17]Copernicus Institute of Sustainable Development, Utrecht University, Utrecht, The Netherlands
[18]School of Earth and Environmental Sciences, University of St Andrews, St Andrews, UK
[19]CONICET – Universidad de Buenos Aires, Centro de Investigaciones del Mar y la Atmósfera (CIMA), Buenos Aires, Argentina
[20]CNRS – IRD – CONICET – UBA. Instituto Franco-Argentino para el Estudio del Clima y sus Impactos (IRL 3351 IFAECI), Buenos Aires, Argentina
[21]Collaborative Innovation Center on Forecast and Evaluation of Meteorological Disasters / Key Laboratory of Meteorological Disaster of Ministry of Education, Nanjing University of Information Science and Technology, Nanjing, China
[22]Centre for Climate Research Singapore, Singapore
[23]Department of Applied Physics and Applied Mathematics, Columbia University, New York, USA

Correspondence: Chaim I. Garfinkel (chaim.garfinkel@mail.huji.ac.il)

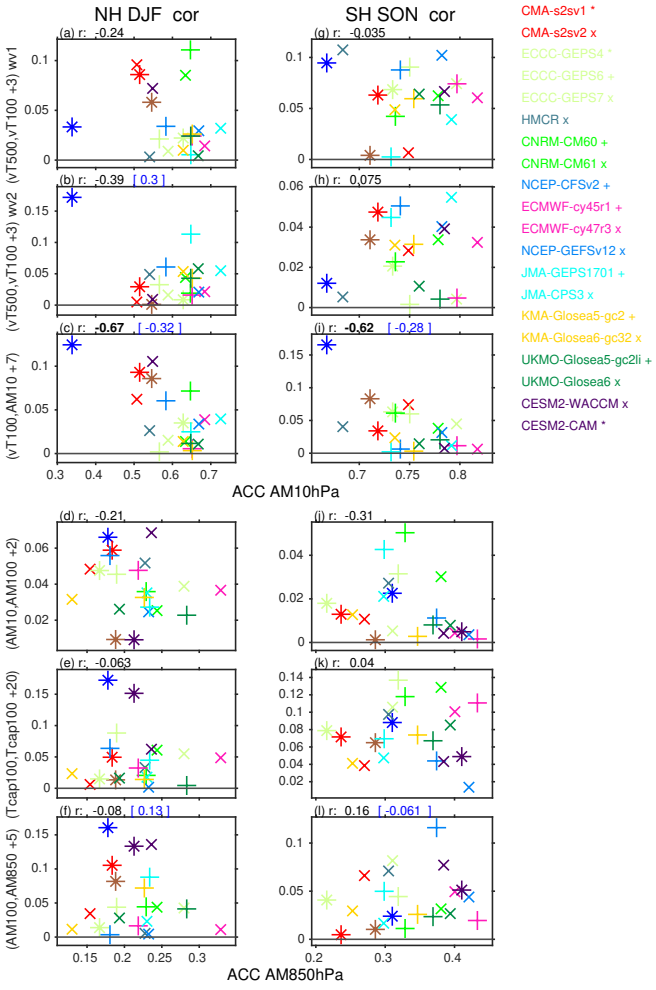


Figure S1. As in Figure 4 in the main text but measuring coupling strength with correlations instead of regressions.

Data availability. The hindcasts from the S2S database used here are available from https://apps.ecmwf.int/datasets/data/s2s/ under the "Reforecasts" S2S set. The NOAA GEFSv12 hindcasts can be obtained from https://registry.opendata.aws/noaa-gefs-reforecast/. Hindcasts for CESM2-CAM are available at https://www.earthsystemgrid.org/dataset/ucar.cgd.cesm2.s2s_hindcasts.html, while those for CESM2-WACCM are from https://www.earthsystemgrid.org/dataset/ucar.cgd.cesm2-waccm.s2s_hindcasts.html. Data for the GFDL-SPEAR can be made available upon request.

Author contributions. CIG and AHB drafted the paper. CIG produced the final version of all figures except Figure 9 and 10. ZDL organized and led the SNAP effort leading to this paper, and also downloaded all of the data. AHB produced the final version of Figure 9 and 10. EDS produced an earlier version of Figures 9 and 10. IS and AYK produced an earlier version of Figure 12. GK produced earlier versions

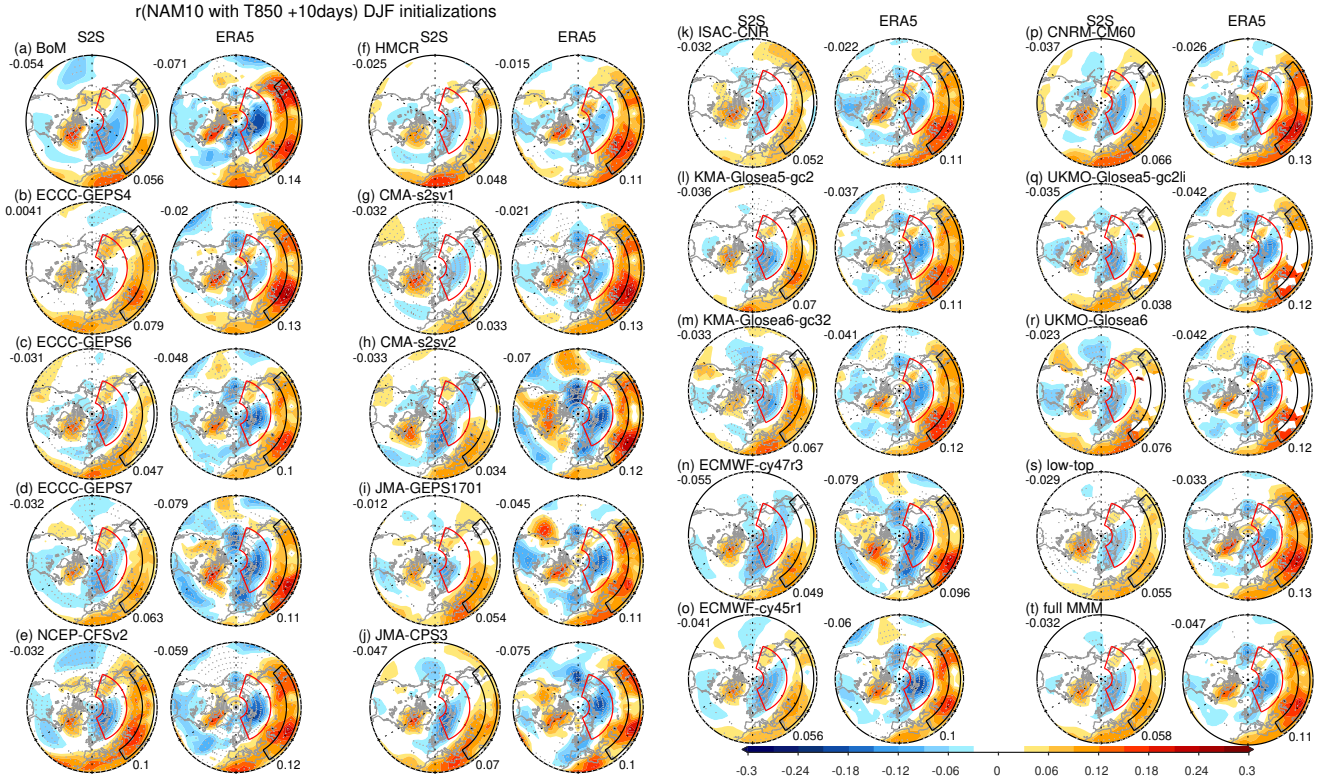


Figure S2. Correlation of NAM10 with T850 lagged by 10 days. T850 is multiplied by -1 to focus on the anomalies associated with a weak vortex. Individual models with available data are shown in panels (a) to (r), the low-top multi-model mean in (s), and the multi-model mean in panel (t). The area-weighted correlation in the red box over Eurasia is shown at the top left for each panel, and at the bottom right for the black box over subtropical Eurasia. Stippling for each model indicates regions where (left column) all available ensemble members indicate the same-signed response, and (right column) all members suffer from the same-signed bias relative to ERA5. Stippling for the low-top and multi-model means (panels s and t) indicates where (left column) all models agree on the sign of the response, and (left column) all models suffer from the same signed bias.

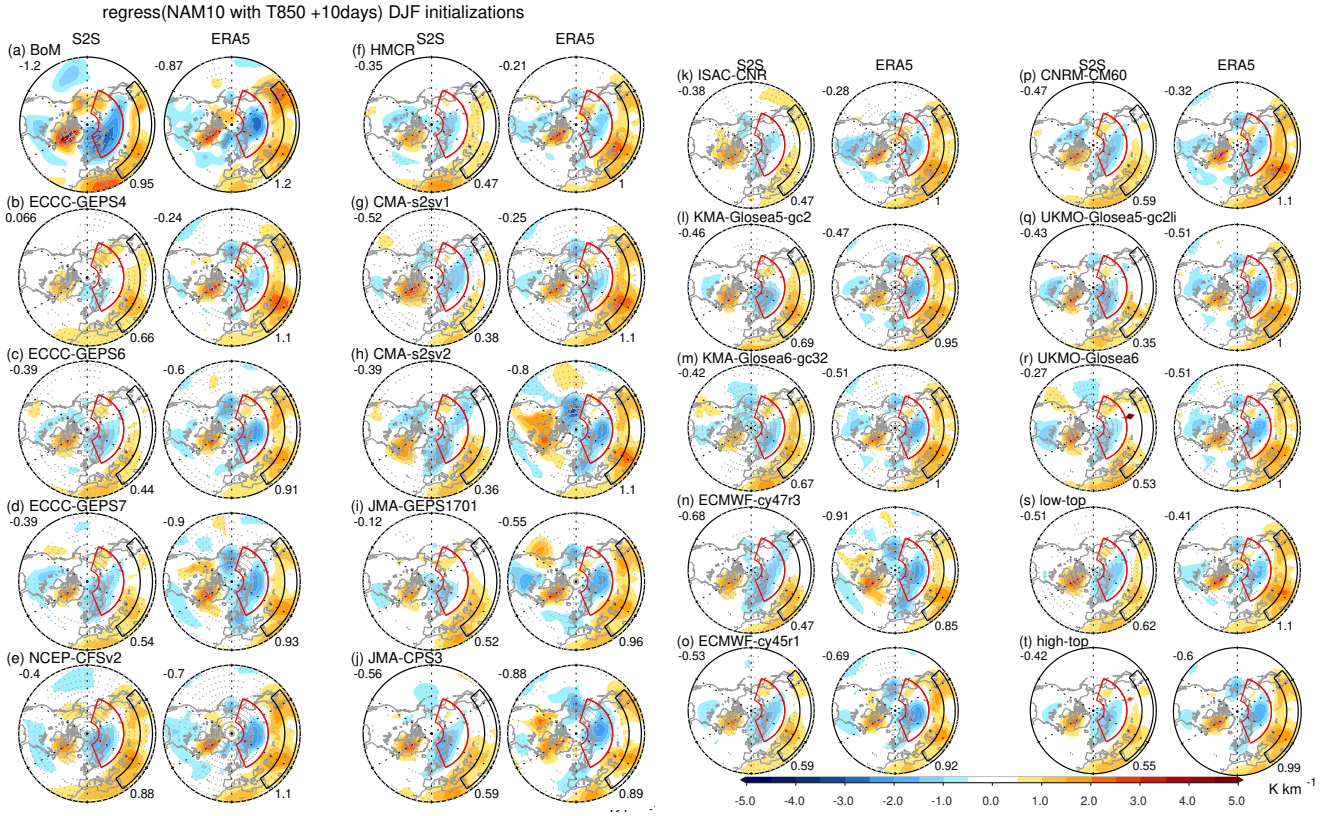


Figure S3. As in Figure S2 but for a regression with T850 lagged by 10 days. The area-weighted correlation in the red box over Eurasia is shown for each panel in the top left, and over subtropical Eurasia in the bottom right.

of Figures 4 and 5. All the listed coauthors were active participants in this SNAP community effort and provided comments on the draft manuscript.

Competing interests. Daniela Domeisen is a member of the editorial board of Weather and Climate Dynamics.

Acknowledgements. This work uses S2S Project data. S2S is a joint initiative of the World Weather Research Programme (WWRP) and the World Climate Research Programme (WCRP). This work was initiated by the Stratospheric Network for the Assessment of Predictability (SNAP), a joint activity of SPARC (WCRP) and the S2S Project (WWRP/WCRP).

The work of R.W. is funded through ETH grant ETH-05 19-1. Support from the Swiss National Science Foundation through projects PP00P2_170523 and PP00P2_198896 to D.D. is gratefully acknowledged. C.I.G and J.R. are supported by the ISF-NSFC joint research program (ISF grant No. 3065/23 and National Natural Science Foundation of China grant no. ????). C.I.G. and J.C. are supported by the NSF-BSF joint research program 355 (United States-Israel Binational Science Foundation grant no. 2021714 and National Science

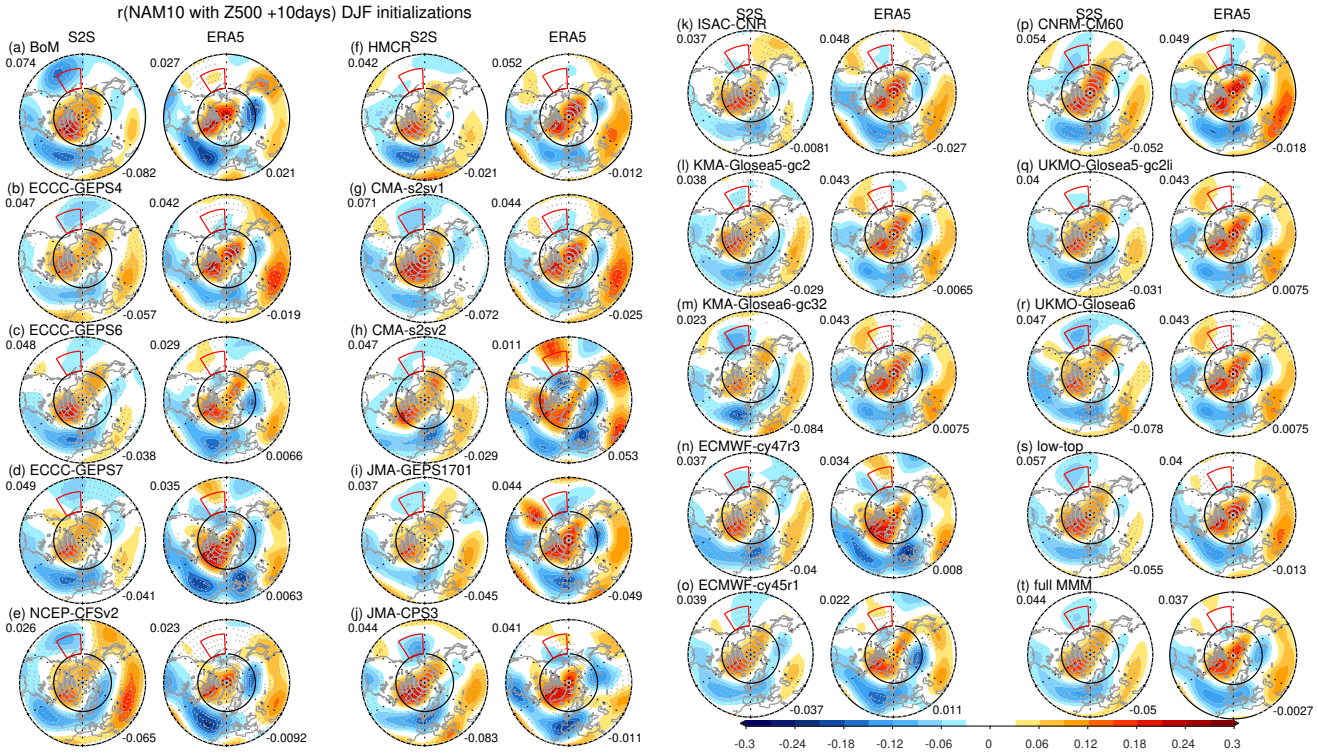


Figure S4. As in Figure S2 but for the correlation of NAM10 with Z500 (latitude vs. longitude) lagged +10 days later. Z500 is multiplied by -1 to focus on the anomalies associated with a weak vortex. The area-weighted correlation over the polar cap is shown in the top left of each panel, and in the North Pacific region with the red box in the bottom right of each panel.

Foundation grant no. AGS-2140909. I.E. and A.Y.K are supported by the Research Council of Finland (grant No. 355792). The work of M.O. is supported by UBACyT 20020220100075BA, PIP 11220200102038CO and PICT-2021-GRF-TI-00498 projects. The work of A.dlC. is funded by the Spanish Ministry of Science through project PID2019-109107GB-I00. B.A and N.C. acknowledge the support of the Spanish Ministry of Science and Innovation through the JeDiS (RTI2018-096402-B-I00) project. FMP and JG-S have been partially supported by the Spanish ATLANTE project (PID2019-110234RB-C21) and "Ramón y Cajal" programme (RYC-2016-21181), respectively. N.P.H. and C.J.W. are supported by UK Natural Environment Research Council (NERC) grant number NE/S00985X/1. C.J.W. is also supported by a Royal Society University Research Fellowship, URF/R/221023. S.-W.S. and H.K. are supported by the National Research Foundation of Korea (NRF) grant funded by the Korean government (MSIT) (2023R1A2C3005607). This material is based upon work supported by the U.S. Department of Energy, Office of Science, Office of Biological & Environmental Research (BER), Regional and Global Model Analysis (RGMA) component of the Earth and Environmental System Modeling Program under Award Number DE-SC0022070 and National Science Foundation (NSF) IA 1947282. This work was also supported by the National Center for Atmospheric Research (NCAR), which is a major facility sponsored by the NSF under Cooperative Agreement No. 1852977. P.L. is supported by award NA18OAR4320123 from the National Oceanic and Atmospheric Administration (NOAA), U.S. Department of Commerce. ZDL was partially supported under NOAA Award

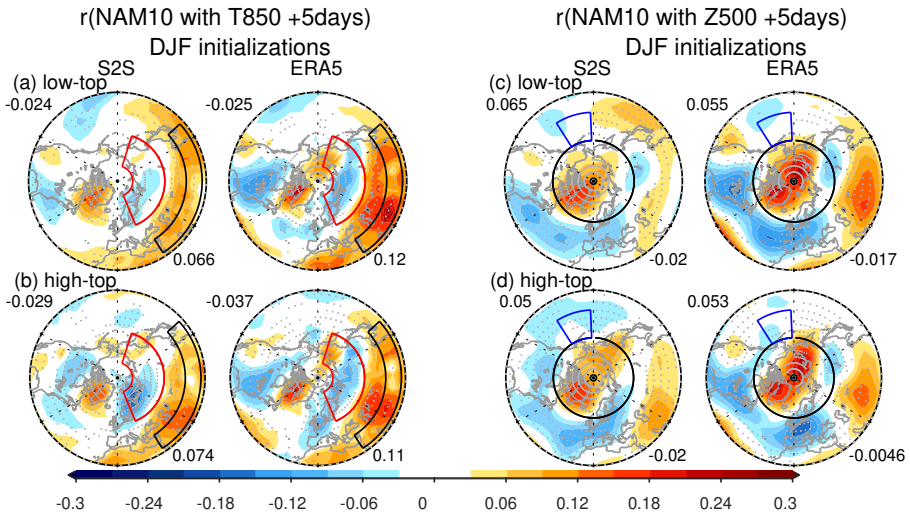


Figure S5. As in Figure 7 in the main text but for the correlation of NAM10 with Z500latlon 5 day later. The area-weighted correlation over the polar cap is shown for each panel.

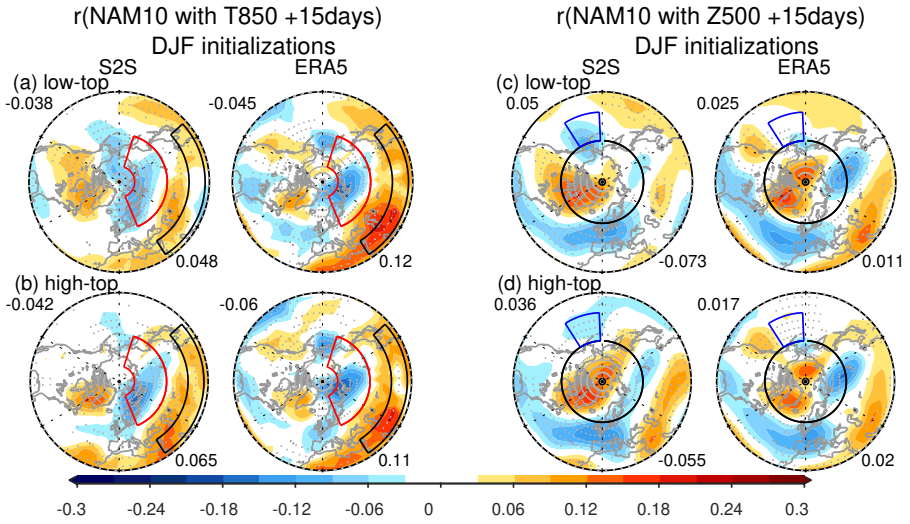


Figure S6. As in Figure 7 in the main text but for the correlation of NAM10 with Z500latlon 15 day later. The area-weighted correlation over the polar cap is shown for each panel.

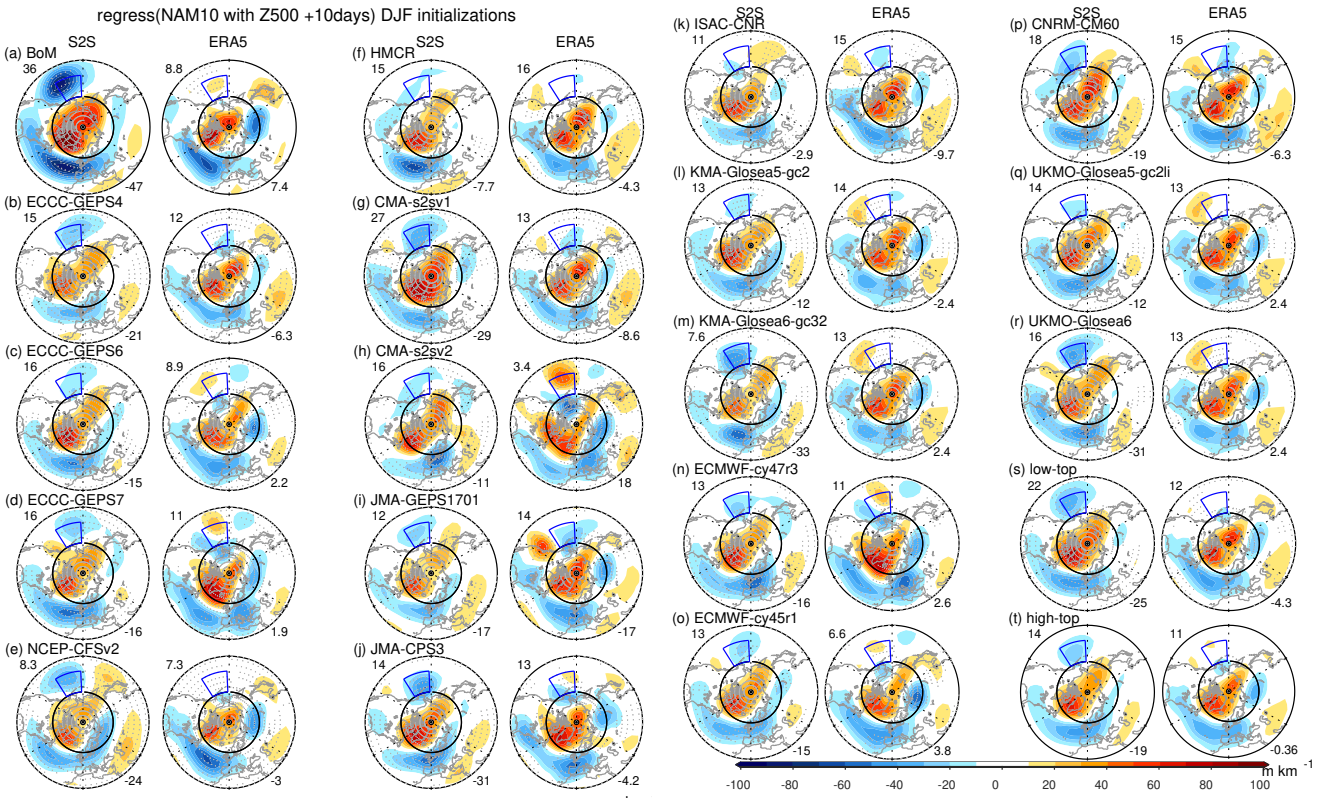


Figure S7. As in Figure S4 but for the regression of NAM10 with Z500latlon lagged +10 days later. The area-weighted regression over the polar cap is shown for each panel in the top left, and over the North Pacific in the bottom right.

NA20NWS4680051; ZDL and JP also acknowledge support from US Federally Appropriated Funds. The statements, findings, conclusions, and recommendations are those of the author(s) and do not necessarily reflect the views of NOAA, or the U.S. Department of Commerce.

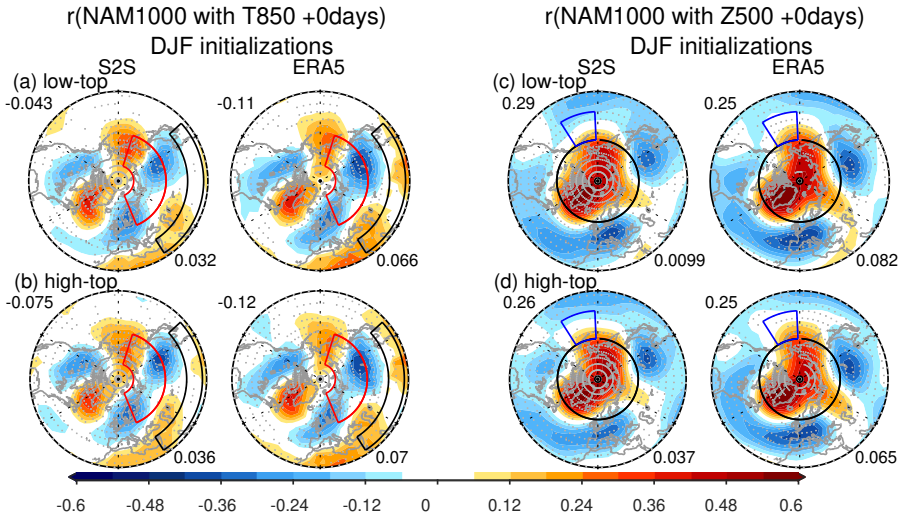


Figure S8. Correlation of NAM1000 with Z500 lagged by 0 days, with NAM1000 taken in days 9 to 12 after initialization. Other plotting conventions follow Figure S4.

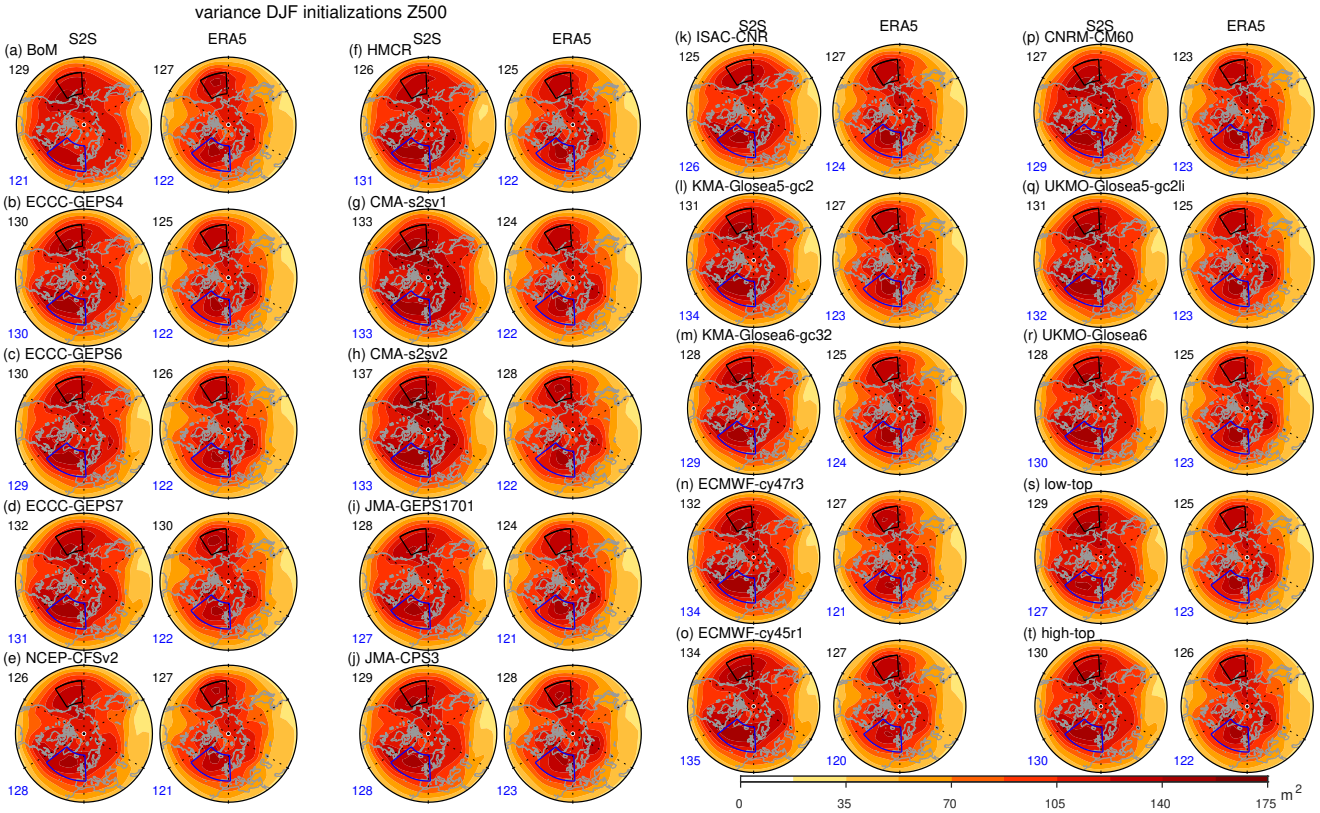


Figure S9. Variance of Z500 in days 22–28 in each system and in ERA5 subsampled to match each system. The area-weighted average in the box over the North Pacific and over the North Atlantic is shown for each panel. The low-top multi-model mean is shown in panel s, and the high-top mean across all 18 models in panel t.

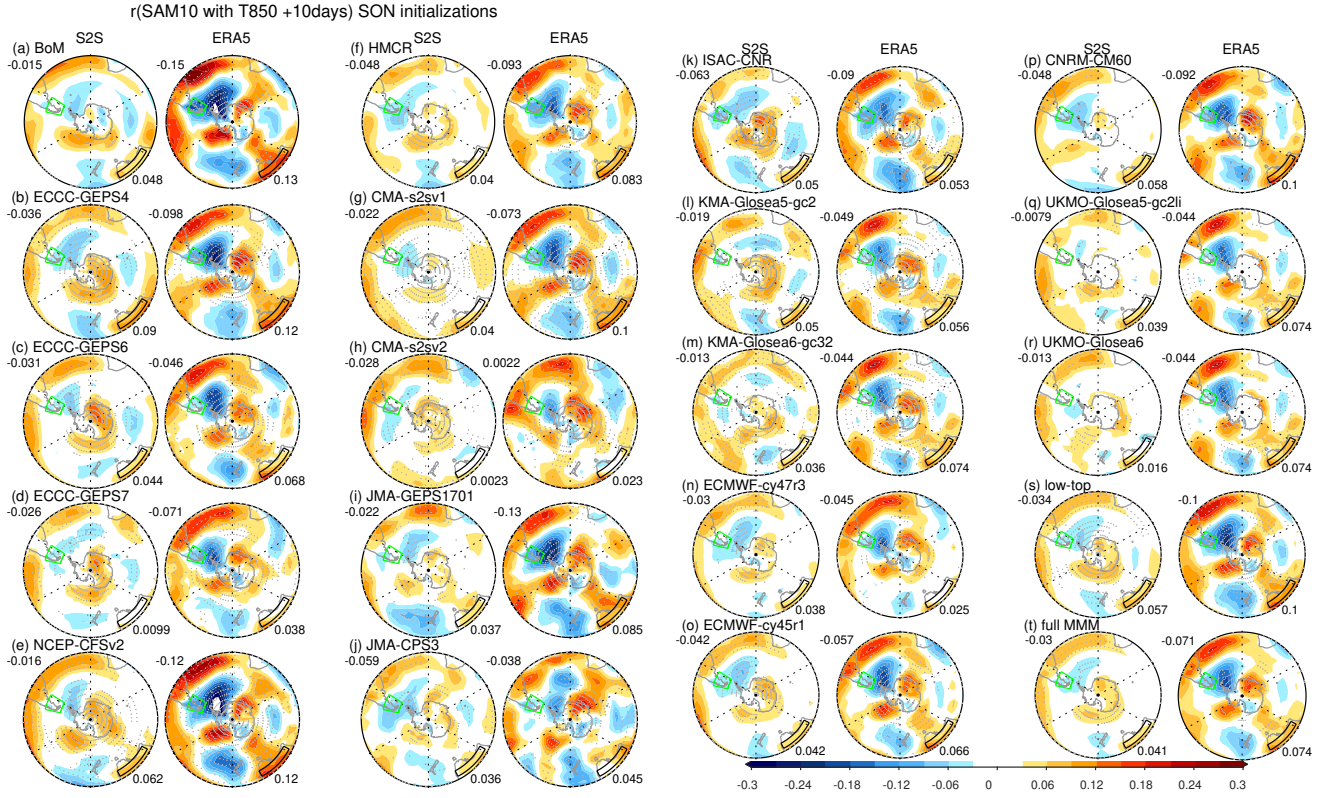


Figure S10. As in Figure S4 but for T850 lagged by 10 days for SH in SON.

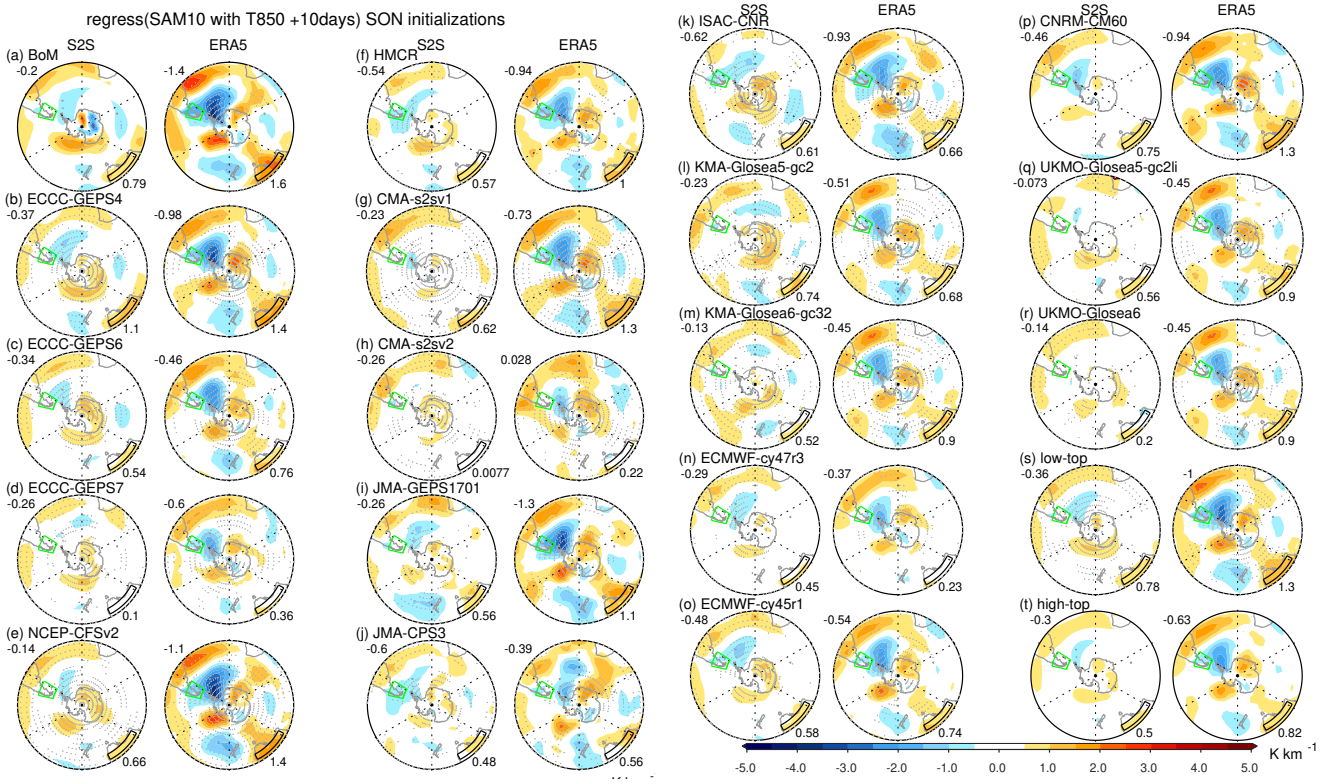


Figure S11. As in Figure S10 but for a regression approach for SH in SON.

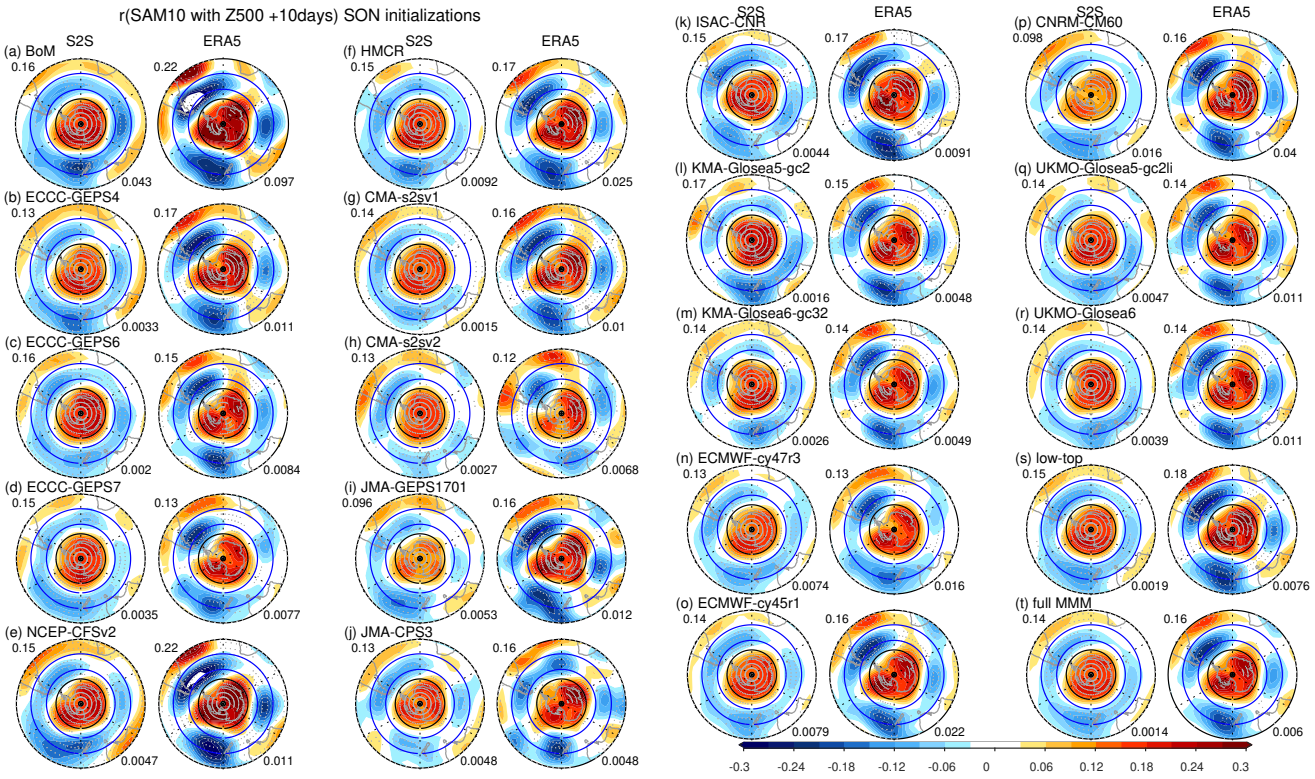


Figure S12. As in Figure S4 but for SH in SON.

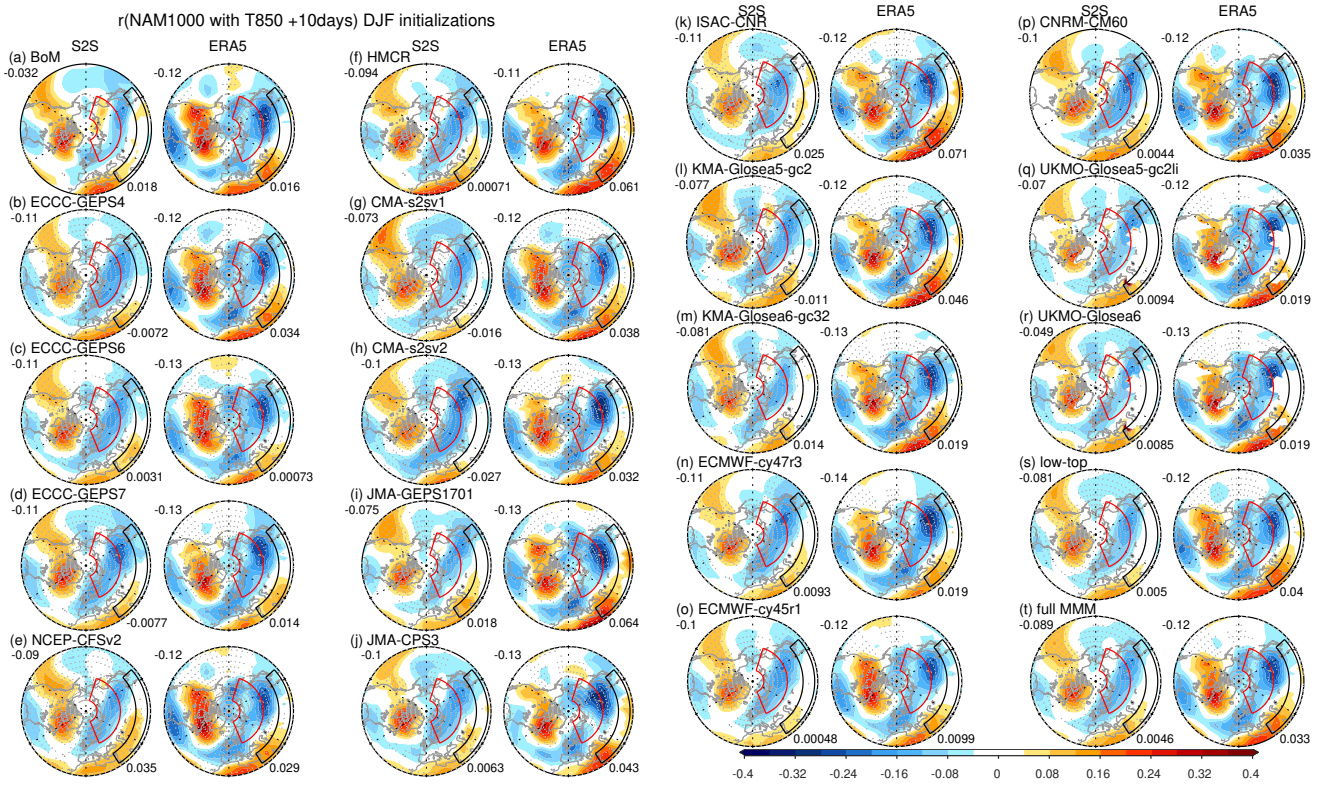


Figure S13. Correlation of NAM1000 with T850 lagged by 10 days, with NAM1000 taken in days 9 to 12 after initialization. Other plotting conventions follow Figure S4 .

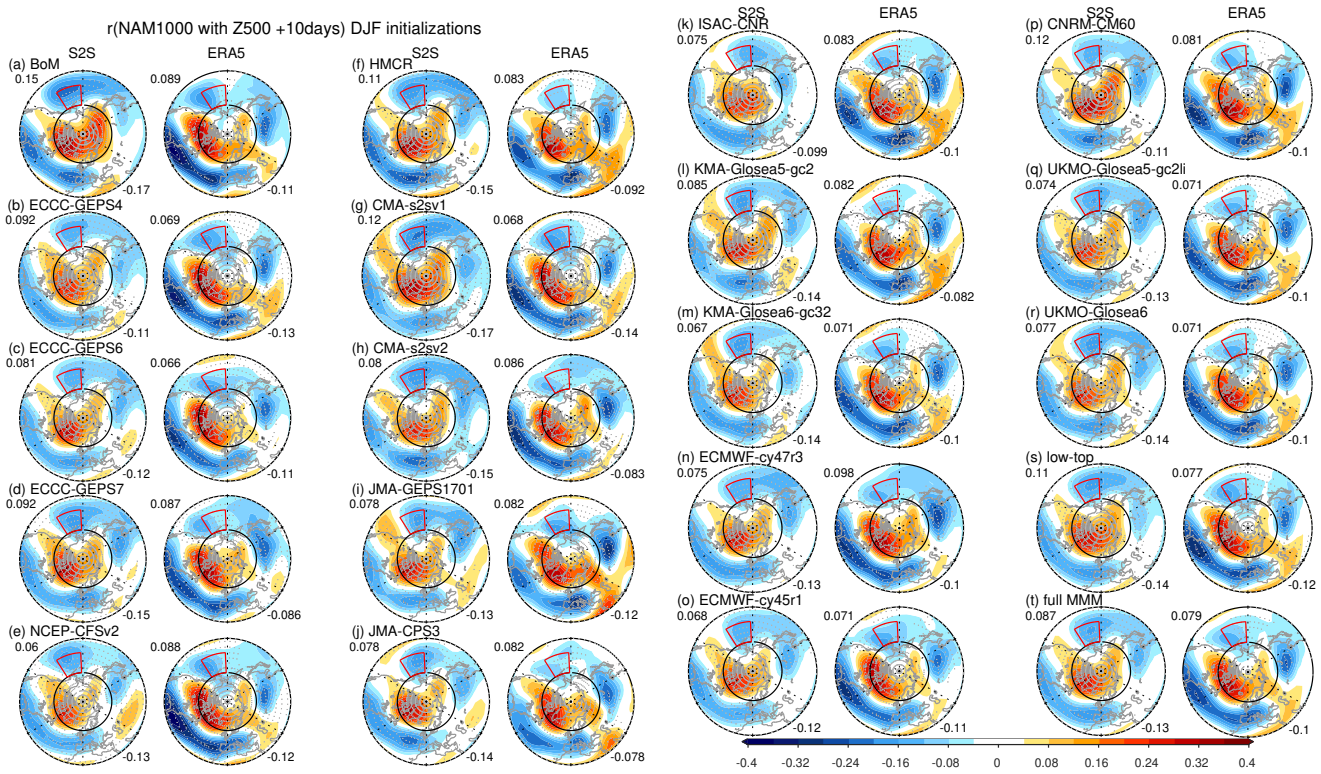


Figure S14. Correlation of NAM1000 with Z500 lagged by 10 days, with NAM1000 taken in days 9 to 12 after initialization. Other plotting conventions follow Figure S4 .

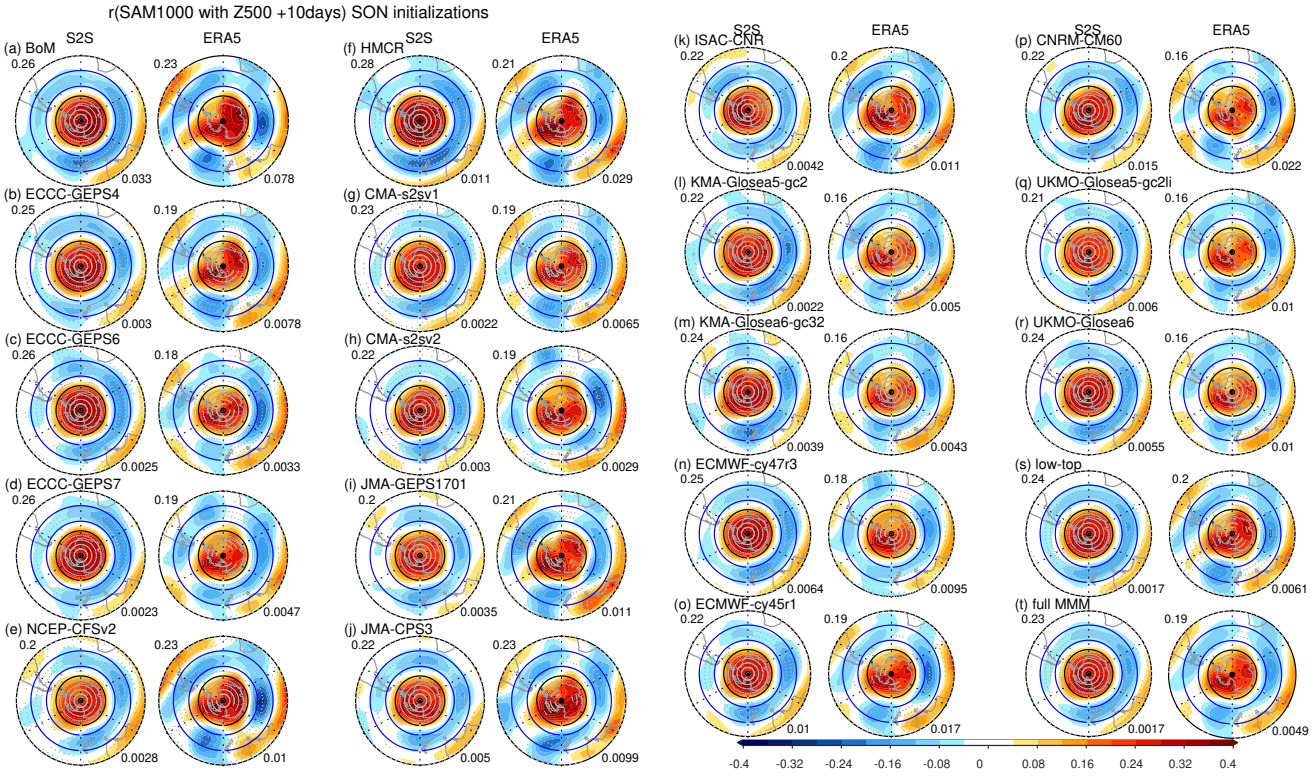


Figure S15. As in Figure S4 but for Z500 lagged by 10 days against SAM1000.